Chinese Journal of Chemical Engineering 67 (2024) 39–48

Contents lists available at ScienceDirect

Chinese Journal of Chemical Engineering

journal homepage: www.elsevier.com/locate/CJChE

Full Length Article

Photoinduced transposed Paternò-Büchi reaction for effective synthesis of high-performance jet fuel

Jinxiu Hu [1, 2, 3, #], Xianlong Liu [1, 2, 3, #], Yi Liu [1], Kang Xue [1, 2, 3, 4], Chengxiang Shi [1, 2, 3, 4], Xiangwen Zhang [1, 2, 3, 4], Li Wang [1, 2, 3, 4], Ji-Jun Zou [1, 2, 3, 4], Lun Pan [1, 2, 3, 4, *]

[1] *Key Laboratory for Green Chemical Technology of the Ministry of Education, School of Chemical Engineering and Technology, Tianjin University, Tianjin 300072, China*
[2] *Haihe Laboratory of Sustainable Chemical Transformations, Tianjin 300192, China*
[3] *Zhejiang Institute of Tianjin University, Ningbo 315201, China*
[4] *Collaborative Innovative Center of Chemical Science and Engineering (Tianjin), Tianjin 300072, China*

ARTICLE INFO

Article history:
Received 21 May 2023
Received in revised form
16 August 2023
Accepted 18 September 2023
Available online 12 December 2023

Keywords:
High-energy-density fuel
Transposed Paternò–Büchi reaction
Kinetics
Bioenergy
Photochemistry

ABSTRACT

High-energy-density fuels are important for volume-limited aerospace vehicles, but the increase in fuel energy density always leads to poor cryogenic performance. Herein, we investigated the transposed Paternò-Büchi reaction of biomass cyclic ketone and cyclic alkene to synthesize a new kind of alkyl-substituted polycyclic hydrocarbon fuel with high energy density and good cryogenic performance. The triplet-energy-quenching results and phosphorescent emission spectra reveal the sensitization mechanism of the reaction, including photosensitizer excitation, triplet-triplet energy transfer, cyclization, and relaxation, and the possible reaction path was revealed by the density functional theory (DFT) calculations. The reaction conditions of photosensitizer type and addition, molar ratio of substrates, reaction temperature, and incident light intensity were optimized, with the target product yield achieving 65.5%. Moreover, the reaction dynamics of the reaction rate *versus* the light intensity are established. After the hydrogenation-deoxygenation reaction, three fuels with a high density of 0.864–0.938 $g \cdot ml^{-1}$ and a low freezing point of < -55 °C are obtained. This work provides a benign and effective approach to synthesize high-performance fuels.

1. Introduction

High-energy-density (HED) fuels, with their high density and high volumetric net heat of combustion (NHOC), are very important for volume-limited aerospace vehicles to extend their flight range [1]. Cycloaddition of cyclic alkene is the most commonly used method to synthesize HED fuels, but higher carbon content leads to poor cryogenic performance (high freezing point and low-temperature viscosity) [2]. Actually, the construction of bicyclic and alkyl-branched structures can realize high density and well-cryogenic properties simultaneously [3–5]. This kind of molecule structure could be obtained by thermal catalytic alkylation, but it seems difficult to synthesize the target products with high yields for the abundant byproducts [6–9].

Alternatively, photoinduced reactions have attracted much attention for their advantages of mild reaction conditions, high product selectivity, and low process energy consumption [10]. Specifically, an efficient C–C coupling process between the ketone and cyclic alkene can produce oxetane products using the [2 + 2] cycloaddition reaction (Paternò–Büchi reaction) triggered by UV light [11–13], whose hydrodeoxygenation can result in the HED fuels with bicyclic and alkyl-branched structures. As for the substrates of HED fuels, the biomass resources attract more attention than the traditional petroleum-derived compounds for their green and sustainable properties [14]. It is worth noting that the cyclic ketones, like cyclohexanone, cyclopentanone, isophorone, *etc.*, can be easily obtained from the degradation and isomerization of lignocellulose [15], which is very promising to be used as the substrate to produce HED fuels.

* Corresponding author.
E-mail address: panlun76@tju.edu.cn (L. Pan).
# These authors contributed to this work equally.

https://doi.org/10.1016/j.cjche.2023.09.014

In this work, we synthesized new alkyl-substituted polycyclic hydrocarbon fuels, *i.e.* *n*-propyl-, cyclopentyl-, or cyclohexyl-substituted norbornane, by photoinduced transposed Paternò-Büchi reaction and hydrogenation deoxygenation reaction, using biomass-derived cyclohexanone and norbornene as substrates. The reaction mechanism was proposed through triplet and phosphorescent quenching tests and density functional theory (DFT) calculations, and the reaction conditions were optimized so that the conversion rate of norbornene (NBE) could reach 85.7% with an oxetane product selectivity of 76.4%. Importantly, the synthesized new-type HED fuel shows high density, a high volume calorific value, and a well-cryogenic property. This work provides a promising and efficient synthetic strategy for HED fuels for practical application.

2. Experimental

2.1. Reagents

NBE, 4,4′-bis(diethylamino)benzophenone, benzophenone, cyclohexene, and 1,3-cyclohexadiene were offered by Shanghai Aladdin Biochemical Technology Co., Ltd, China. Acetophenone (AP) was provided by Tianjin Heowns Biochemical Technology Co., Ltd, China. Xanthone and cyclopentene were brought from Meryer (Shanghai) Chemical Technology Co., Ltd, China. Cyclohexanone (CHO), cyclopentanone (CPO), and 2-butanone were supplied by Tianjin Jiangtian Chemical Technology Co., Ltd, China. Acetone (ATO), trans-stilbene (TS), cyclohexane, and dichloromethane were purchased from Tianjin Yuanli Chemical Co., Ltd, China. HY (SiO_2/Al_2O_3 = 5.4) was brought from Nankai Catalysts Co. (China), and 5% (mass) Pd/C was provided by Tianjin Sinoopod Technology Co., Ltd, China.

2.2. Photoinduced transposed Paternò-Büchi reaction

The photoinduced transposed Paternò-Büchi reaction (intermolecular [2 + 2] cycloaddition) was performed in a 50-ml quartz glass tube under 365 nm LED irradiation. First, the cyclic ketone, cyclic alkene, and photosensitizer were mixed into the reactor and then soaked with helium for 30 min under constant stirring. Then, the reaction was conducted under light irradiation for 10 h at a specific temperature (−10–20 °C) and incident light flux (50–130 mW·cm^{-2}). After the reaction was completed, the solution was qualitatively analyzed by using an Agilent 6890/5975 gas chromatography-mass spectrometer (equipped with an HP-5 capillary column) and an NMR spectrometer, and quantitatively analyzed by using a gas chromatograph (Agilent-7820A) with an FID detector and an HP-5 capillary column using the internal standard method. The correction factor of each substrate was measured with paraxylene as an internal standard, and the values for NBE, CHO, and AP are 0.9728, 1.0115, and 1.1125, respectively. The reaction parameters can be calculated using the following formulas:

$$\text{Conversion} = \frac{m(\text{reactant converted})}{m(\text{original reactant})} \times 100\% \quad (1)$$

$$\text{Selectivity} = \frac{m(\text{target product produced})}{m(\text{reactant converted})} \times 100\% \quad (2)$$

$$\text{Yield} = \frac{m(\text{target product produced})}{m(\text{original reactant})} \times 100\% \quad (3)$$

The hydrogenation deoxygenation (HDO) reaction of photosynthesized oxetane products was conducted in 500-ml autoclaves with mechanical agitation, using Pd/C-HY as a catalyst. Then, the new-type HED fuels were obtained through filtration, rotary evaporation, and vacuum distillation.

2.3. Measurements of fuel properties

The fuel density was measured by using a Mettler Toledo DE40 densitometer at a reaction temperature of 20 °C. The net heat of combustion (NHOC) of fuel was measured using an IKA-C6000 isoperibol package 2/10 calorimeter. The kinematic viscosity and freezing point of fuel were determined based on ASTM D445 and ASTM D2386, respectively.

2.4. Theoretical calculations

All the geometry optimizations and frequency calculations of reactant, product, intermediate (INT), and transition states (TS) were performed at B3LYP levels of theory along with the 6-311G (d, p) basis set, which includes polarization functions on all atoms except hydrogen atoms. The transition state search has been optimized using Berny's algorithms [16]. A single-point frequency calculation was carried out to make sure the transition states contained only imaginary frequencies. Intrinsic reaction coordinate (IRC) calculations are conducted to ensure that the transition states connect to the correct reactants and intermediates/products [17]. All the calculations were performed using the GAUSSIAN 09 package of programs (see Fig. 1).

3. Results and Discussion

3.1. Reaction pathway for transposed Paternò-Büchi reaction

As shown in Fig. 2(a), the mixture of NBE and CHO (molar ratio of 1:4) without photosensitizer shows very low [2 + 2] cycloaddition reaction conversion, *i.e.* 7.5% for NBE and 1.8% for CHO, under 365 nm light irradiation for 10 h. This is because the light absorption edges of NBE and CHO are both less than 350 nm (Fig. 2(b), which cannot effectively absorb and convert the energy of 365 nm light. Then, the commonly used photosensitizer AP, with strong light absorption (Fig. 2(b)), was applied to sensitize this [2 + 2] cycloaddition reaction. In Fig. 2(a), the AP addition significantly increases the conversions of NBE and CHO to 85.7% and 18.0%, respectively, with a high selectivity of 76.4% for the oxetane products (the mass spectra are shown in Fig. S1, Supplementary Material), whose decline compared to the AP-unadded case is attributed to the byproducts, as shown in Fig. 2(c), which include norbornane, the dimerization product of NBE itself [18], and the cycloaddition product between NBE and AP (whose distribution over time is shown in Fig. 2(d) and the mass spectra are shown in Fig. S4). The above results effectively illustrate the photosensitization effect of AP on [2 + 2] cycloaddition.

Then, the triplet quenching and phosphorescence quenching experiments were performed to understand the mechanism of the photoinduced cycloaddition reaction. Numerous studies have confirmed that α,β-unsaturated cyclic ketones can sensitize the *cis*-trans isomerism of the alkene *via* the transfer of triplet state energy [19–21]. Therefore, *trans*-stilbene (TS) with lower triplet energy (about 50 kcal·mol^{-1}, 1 kcal·mol^{-1}= 4.18 kJ·mol^{-1}) was used as a triplet quencher to prove the presence of the triplet AP (about 78 kcal·mol^{-1}). As shown in Fig. 3(a), the addition of TS significantly decreases the NBE conversion from 85.7% to 13.1%, and the conversion of CHO is as low as 3.7%. Especially, a *cis*-stibene

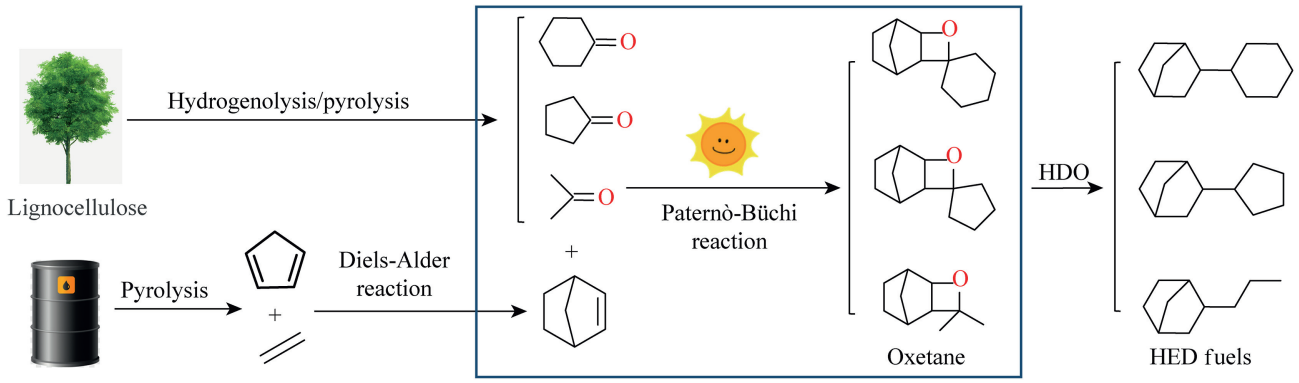

Fig. 1. Synthesis pathway of new-type HED fuels *via* the transposed Paternò-Büchi reaction and hydrogenation deoxygenation reaction.

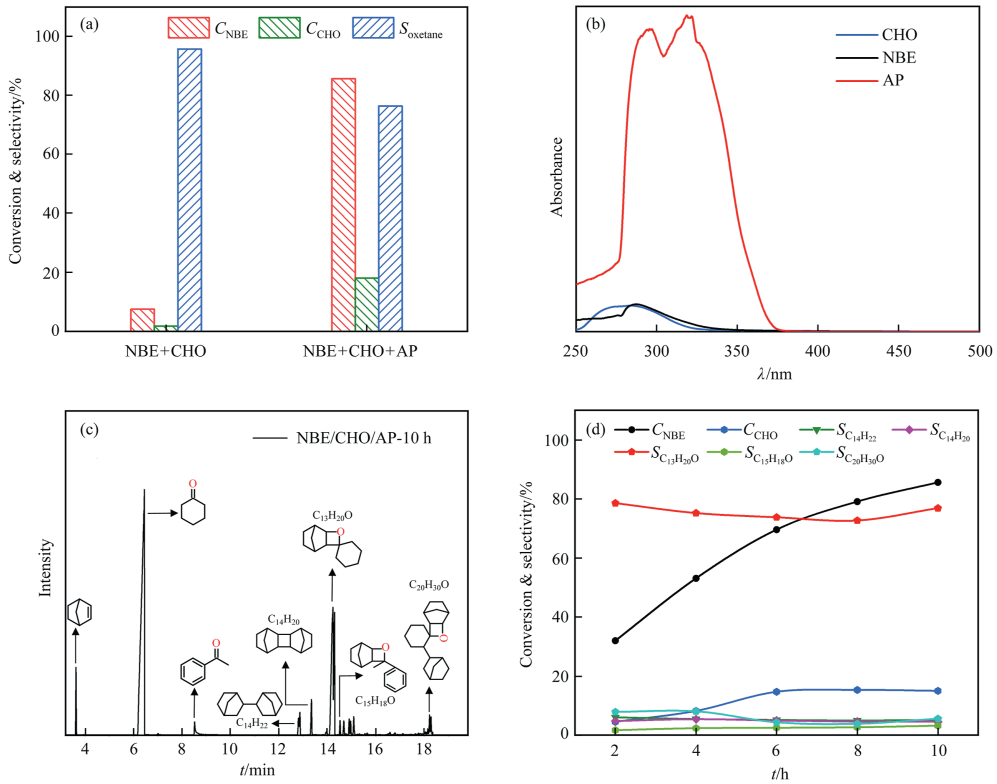

Fig. 2. (a) Effect of AP addition on cycloaddition reaction performance (10 h, 20 °C, 130 mW·cm^{-2}, the molar ratio of NBE/CHO is 1: 4, and AP was added at 10% (mol) of NBE). (b) UV–vis absorption spectra of NBE, CHO, and AP. (c) GC spectra of product distribution. (10 h, 20 °C, 130 mW·cm^{-2}, the molar ratio of NBE/CHO is 1: 4, and AP was added at 10% (mol) of NBE). (d) Time-dependent photoinduced cycloaddition of NBE and CHO sensitized by AP.

byproduct was detected by gas chromatography at the end of the reaction (as shown in Fig. 3(b)), which must be obtained by triplet energy transfer of AP because the *trans*-stilbene cannot be directly excited by UV excitation to undergo *cis*-deactivated isomerism [22]. As shown in the phosphorescent emission spectra (the red line in Fig. 3(c)), AP excited by light will form a triplet state, which releases phosphorescent light when it relaxes to the ground state. The above experimental results strongly prove the existence of a triplet energy transfer process.

The specific mechanism of energy transfer of triplet AP to the reaction substrate (NBE or CHO) can be verified by phosphorescent quenching reactions. Actually, CHO cannot obtain the energy of triplet AP for its too high triplet energy (78 kcal·mol^{-1}); however, higher concentration of NBE allows for more efficient quenching of AP (as shown in Fig. 3(c)). This result shows that the triplet AP transfers energy to NBE for the next reaction, which is in line with the previous results [18]. Based on the different sensitization order from the traditional Paternò-Büchi reaction, this reaction should be called the transposed Paternò-Büchi reaction [11–13].

It has been indicated that the photoinduced cycloaddition reaction, realized *via* the triplet-triplet energy transfer between the photosensitizer and the substrate, involves the formation of a double-radical intermediate [23]. Therefore, a possible reaction path for the transposed Paternò-Büchi reaction between NBE and CHO was proposed, as shown in Fig. 4. Firstly, AP absorbs photon energy and is excited to the singlet state A after being irradiated by the 365 nm light, and the excited state A converts to the excited triplet state B through the intersystem crossing (ISC) process, or relaxes to the ground state. Secondly, triplet B transfers energy to the ground NBE through the triplet–triplet energy transfer (TTET)

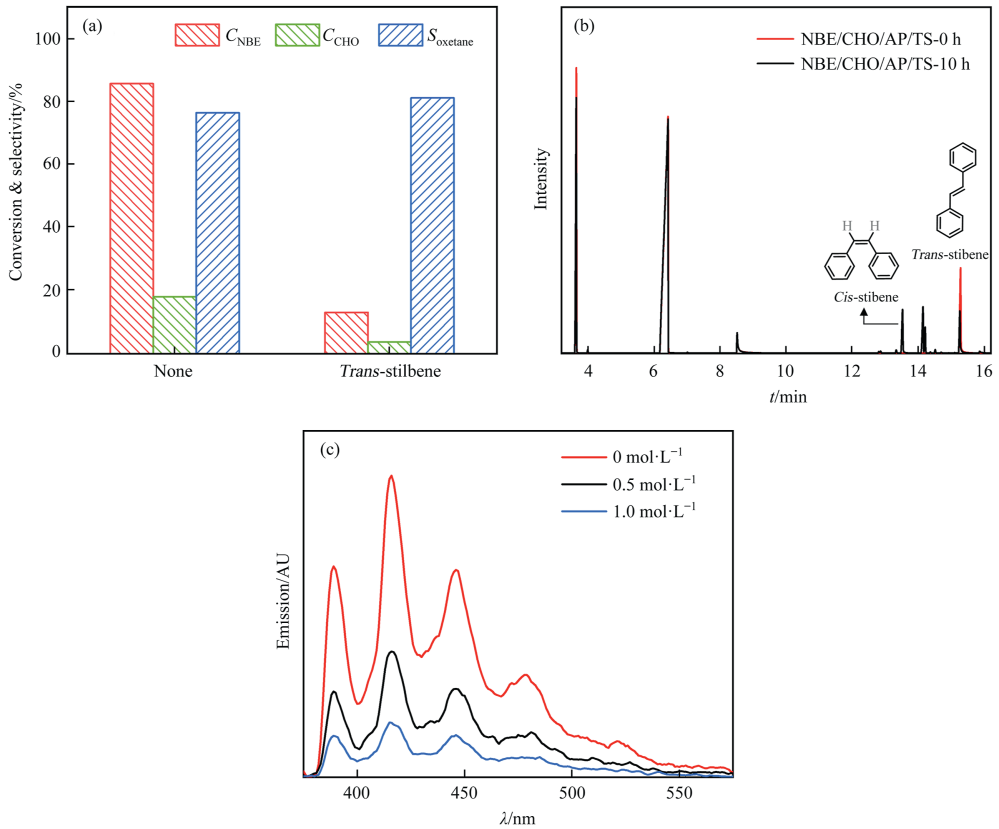

Fig. 3. (a) Effect of *trans*-stilbene on cycloaddition reaction of NBE and CHO photosensitized by AP (10 h, 20 °C, 130 mW·cm^{-2}, the molar ratio of NBE/CHO is 1: 4, AP and TS were added at 10% (mol) of NBE). (b) Typical chromatograms before and after the addition of the *trans*-stilbene. (c) Effect of different concentrations of NBE on the phosphorescent emission spectra of AP. (Toluene, 365 nm, −196.15 °C, the concentration of AP is 0.1 mol·L^{-1}).

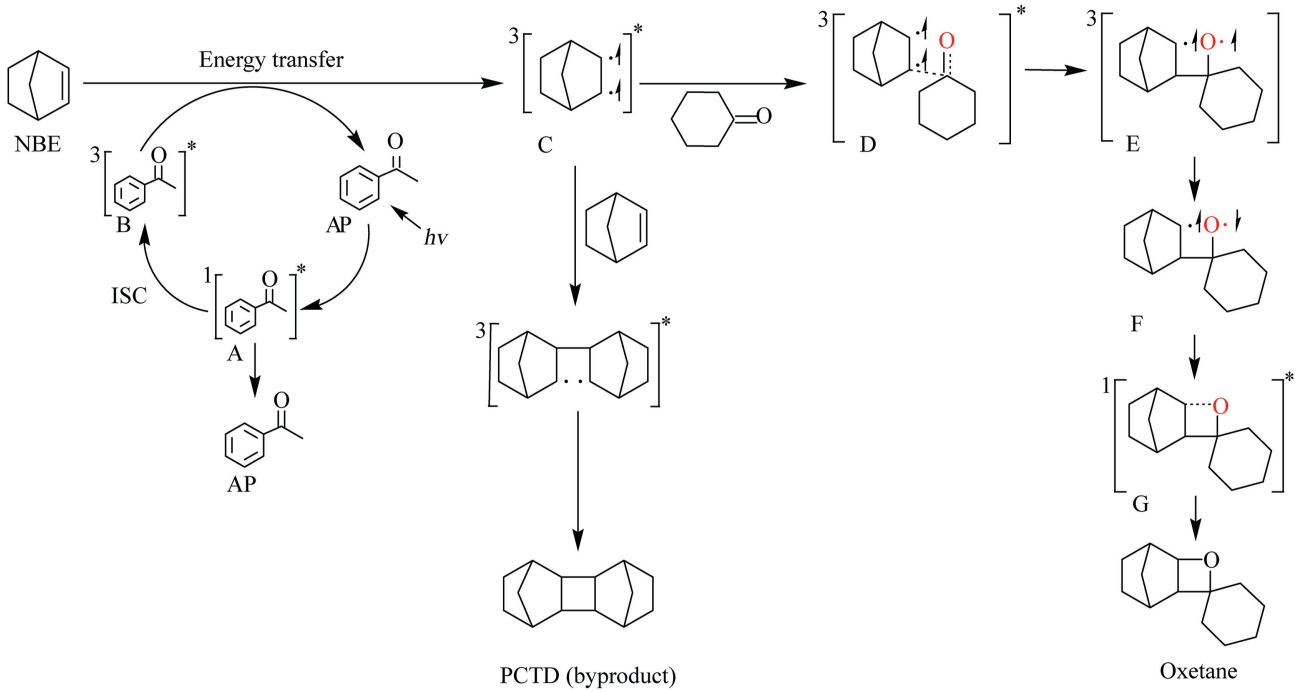

Fig. 4. Proposed reaction pathway of transposed Paternò-Büchi reaction between NBE and CHO photosensitized by AP.

process, generating excited triplet NBE (C), with B relaxing to the ground state (AP). After that, C collides with the ground state CHO to form a reactive complex (D) that further transforms into the excited compound in the transition state (E), and subsequently the excited complex will form a double radical intermediate (F) [12], which decays through the transition state (G) to form the oxetane product. In addition, the main byproduct is the intermolecular cycloaddition product of the NBE (PCTD), which is generated by the collision between the triplet NBE (C) and the ground-state NBE [18].

To further investigate the energy profile of the transposed Paternò-Büchi reaction between NBE and CHO, the DFT calculation was conducted to generate a simplified energy profile using the ground state CHO + NBE energy barrier as a reference (Fig. 5). The NBE requires uphill Gibbs free energy of 72.77 kcal·mol^{-1} (which is lower than the triplet-state energy of AP, *ca.* 78 kcal·mol^{-1}) to be excited from the ground state to the first triplet state (T1). The two spin-parallel electrons of T1 are mainly populated at the C2 and C3 positions of the norbornane ring, with an elongated C2–C3 bond (0.151 nm). Then, the next step, C–C bond formation between the C2 (or C3) of the norbornane ring and the carbonyl group of cyclohexanone *via* TS1, has a high energy of 89.61 kcal·mol^{-1}. The subsequent intersystem crossing from triplet diradical INT1 (71.05 kcal·mol^{-1}) to the corresponding open-shelled singlet diradical species INT1-OSS (69.65 kcal·mol^{-1}) occurs *via* inter-system crossing (ISC). At last, the energetically feasible radical–radical combination happens *via* the transition state TS2 (79.13 kcal·mol^{-1}) and relaxing to the [2 + 2] cycloaddition product (17.71 kcal·mol^{-1}). Since there is no C3-alkyl substituent in NBE, the [2 + 2] cycloaddition toward products is the only available reaction pathway [24].

3.2. The effect of photosensitizer type on the transposed Paternò-Büchi reaction

Adding the photosensitizer to absorb light energy and thus promote the transposed Paternò-Büchi reaction (which cannot be directly motivated by the light) is necessary and effective. Organic ketone photosensitizers with the characteristics of low cost, easy separation, high triple energy, and long life are commonly considered for the cycloaddition reaction of alkenes. The type and concentration of photosensitizers significantly affect the photoinduced cycloaddition reaction, and the appropriate photosensitizer can effectively initiate the reaction [25–27]. In this work, several

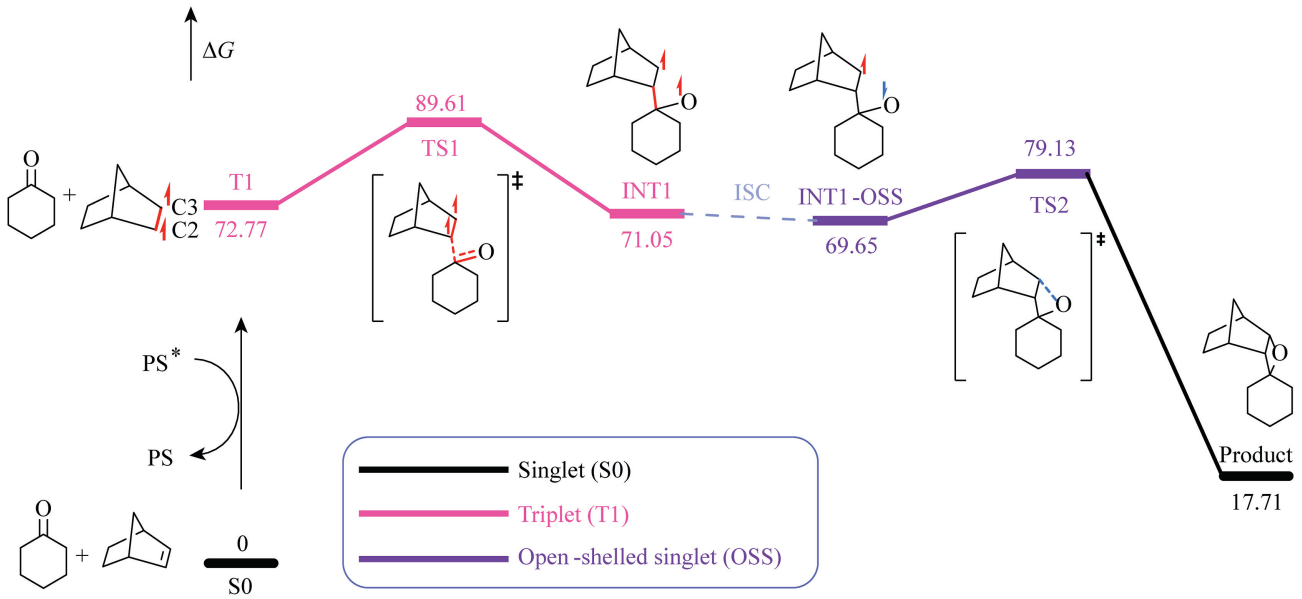

Fig. 5. Energy profile of the Paternò–Büchi [2 + 2] cycloaddition. Calculated at the (U)B3LYP/6-311G(d,p) level of theory. The Gibbs free energies (ΔG) are in kcal·mol^{-1}. The unpaired electrons with different spins are marked by colored arrows (alpha spin in red, beta spin in blue).

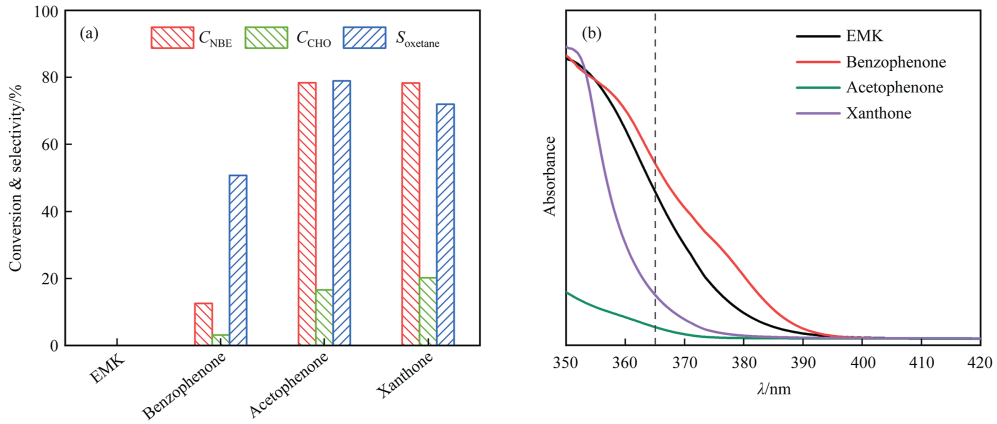

Fig. 6. (a) Effect of different photosensitizers on transposed Paternò-Büchi reaction between NBE and CHO (10 h, 20 °C, 130 mW·cm^{-2}, the molar ratio of NBE/CHO is 1: 4, photosensitizer was added at 5% (mol) of NBE), (b) UV–vis absorption spectra of different photosensitizers.

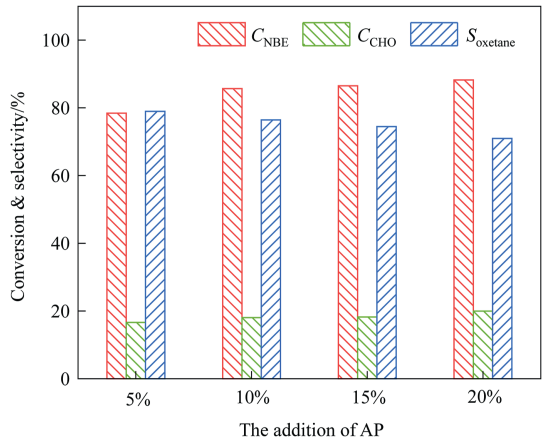

Fig. 7. Effect of AP molar amount on transposed Paternò-Büchi reaction between NBE and CHO (10 h, 20 °C, the molar ratio of NBE/CHO is 1: 4, 130 mW·cm^{-2}).

common ketone photosensitizers, including 4,4′-bis (diethylamino) benzophenone (EMK), benzophenone, AP, and xanthone, were utilized to demonstrate the effects of photosensitizer type and concentration on the reaction. As shown in Fig. 6(a), no NBE and CHO are converted in the presence of EMK. Both NBE and CHO conversions are very low (12.5% and 3.1%, respectively) when using benzophenone as a photosensitizer, and the oxetane selectivity is only 50.7%, ascribing to the side Paternò-Büchi reaction between NBE and benzophenone. AP and xanthone show relatively higher photosensitized reactivity, with the NBE conversions reaching 78.4% and 78.3%, the CHO conversions reaching 16.6% and 20.2%, and the oxetane selectivity up to 78.9% and 72.0%, respectively.

Fig. 6(b) shows the UV-visible absorption spectra of different photosensitizers. Although EMK shows strong light absorption at 300–375 nm (the UV-visible absorption spectra at 300–350 nm are shown in Fig. S5), it cannot initiate the reaction because its triplet energy of 64 kcal·mol^{-1} [28] is far lower than that of NBE (74 kcal·mol^{-1}) [18]. The sensitized reactivity of benzophenone is very low (the conversion of NBE is only 12.5% and the yield of oxetane is only 6.34%), which is probably due to the slightly lower triplet energy (69 kcal·mol^{-1}) [29,30] than NBE. AP and xanthone show higher triplet energy than NBE, which can effectively sensitize NBE to an excited state with a high conversion. Among the above photosensitizers, the AP-sensitized reaction shows the highest reactant conversion and target product selectivity, so AP is chosen as the optimal photosensitizer for subsequent reactions.

The effect of the photosensitizer amount was explored, and the results are shown in Fig. 7. As the gradual increase of AP addition increases from 2.05 mmol (5%) to 8.2 mmol (20%), the NBE (CHO) conversion increases from 78.4% (16.6%) to 88.2% (20.0%), while the oxetane selectivity decreases from 78.9% to 70.9%. The higher AP concentration can accelerate the TTET process and improve the reaction conversion, but it also significantly increases the collision between NBE and NBE (or AP), producing more by-products and decreasing the target product selectivity. Fig. 7 shows that the optimal addition of AP is 10%, under which the oxetane yield can reach the highest (*ca.* 65.5%).

3.3. Optimization of photoreaction conditions

In addition to the photosensitizer, the other reaction conditions, including incident light flux (Q), reaction temperature (T), and the NBE/CHO ratio, were then optimized. As shown in Fig. 8(a), when increasing the light flux from 50 mW·cm^{-2} to 170 mW·cm^{-2}, the

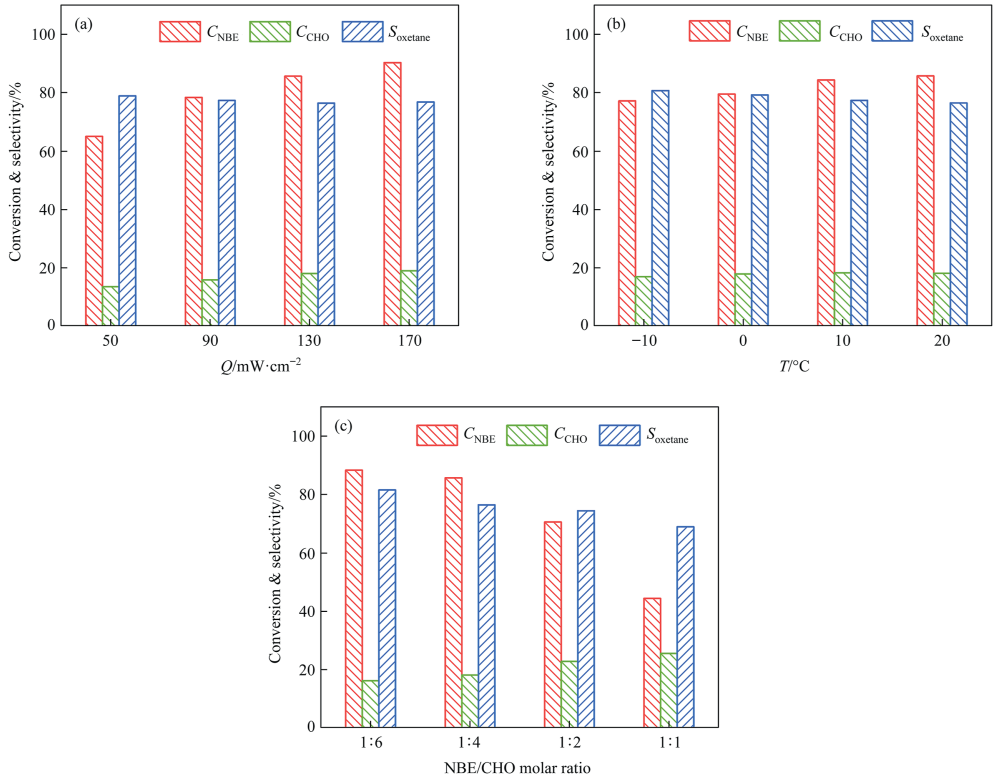

Fig. 8. Effects of (a) light flux (10 h, 20 °C, the molar ratio of NBE/CHO is 1: 4, AP was added at 10% (mol) of NBE), (b) reaction temperature (10 h, 130 mW·cm^{-2}, the molar ratio of NBE/CHO is 1: 4, AP was added at 10% (mol) of NBE), and (c) NBE/CHO molar ratio (10 h, 20 °C, 130 mW·cm^{-2}, the addition of AP is 10% and the total mass of substrates is 20 g) on transposed Paternò-Büchi reaction between NBE and CHO.

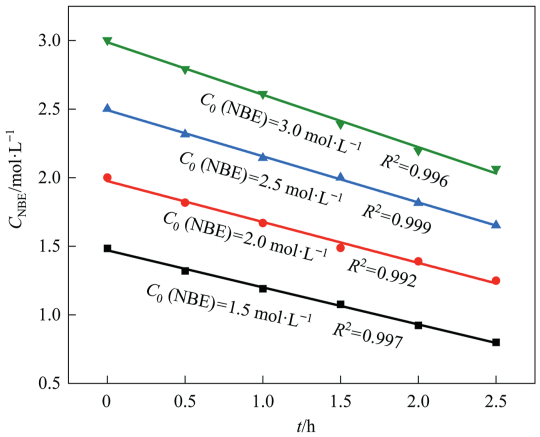

Fig. 9. Fitted curves for NBE concentration and illumination time under different initial substrate concentrations (130 mW·cm^{-2}, 20 °C, 10 h).

NBE conversion increases significantly from 65.0% to 90.3%, and the oxetane selectivity slightly reduces from 78.9% to 76.8%. Therefore, a larger light flux can lead to higher product yield. But considering the lifetime of the light source (which will be significantly reduced by too much light flux), we chose 130 mW·cm^{-2} as the optimal light flux.

The influence of reaction temperature on the transposed Paternò-Büchi reactivity is exhibited in Fig. 8(b). With the temperature gradually increasing from −10 °C to 20 °C, the NBE (CHO) conversion increases from 77.1% (16.9%) to 85.7% (18.0%), but the oxetane selectivity decreases from 80.7% to 76.4% because the high temperature makes the double-radical intermediates unstable (formed by the triplet NBE with CHO) [12]. Overall, the temperature has very little effect on the product yield, so the room temperature of 20 °C is chosen as the applied temperature.

According to Fig. 8(c), with the increasing molar ratio of NBE/CHO (from 1: 6 to 1: 1), the conversion of NBE decreases from 88.3% to 44.4%, the CHO conversion slightly increases from 16.2% to 25.5%, and the oxetane selectivity drops from 81.5% to 68.9%. This is explained by the fact that a higher CHO content can reduce the probability of an intramolecular reaction of NBE to inhibit the formation of by-products. However, a too low NBE/CHO ratio causes the waste of CHO. Therefore, the NBE/CHO ratio of 1:4 is chosen.

3.4. Kinetics of transposed Paternò-Büchi reaction

To explore the kinetic equations, a series of experiments under different incident light intensities (Q) and substrate concentrations were conducted. The kinetic equations of the reaction process were derived as follows:

$$r_{\text{oxetane}} = \frac{\mathrm{d}C_{\text{oxetane}}}{\mathrm{d}t} = KC_{\text{NBE}}^{\alpha}C_{\text{CHO}}^{\beta} \tag{4}$$

where r_{oxetane} is the generation rate of oxetane, mol·L^{-1}·h^{-1}; C_{oxetane}, C_{NBE}, and C_{CHO} indicate the concentrations of oxetane, NBE, and CHO, respectively, mol·L^{-1}; t represents the reaction time, h; K is the rate constant; α and β indicate the reaction series of NBE and CHO, respectively.

Due to the excess of cyclohexanone for this reaction, Eq. (4) can be simplified to the following formulas:

$$r_{\text{oxetane}} = \frac{\mathrm{d}C_{\text{oxetane}}}{\mathrm{d}t} = K^{*}C_{\text{NBE}}^{\alpha} \tag{5}$$

$$K^{*} = KC_{\text{CHO}}^{\beta} \tag{6}$$

$$\frac{\mathrm{d}C_{\text{oxetane}}}{\mathrm{d}t} = -\frac{\mathrm{d}C_{\text{NBE}}}{\mathrm{d}t} \times S \tag{7}$$

where K* indicates the rate constant and S is oxetane selectivity.

Then, Eqs. (8) and (9) can be derived from the above formulas.

$$\ln(r_{\text{oxetane}}) = \ln\left(-\frac{\mathrm{d}C_{\text{NBE}}}{\mathrm{d}t} \times S\right) = \ln(K^{*}) + \alpha \ln(C_{\text{NBE}}) \tag{8}$$

$$\ln(r_{\text{oxetane}}) - \alpha \ln(C_{\text{NBE}}) = \ln(K) + \beta \ln(C_{\text{CHO}}) \tag{9}$$

The transposed Paternò-Büchi reactions with different concentrations of the initial substrate were carried out with a fixed light flux of 130 mW·cm^{-2}. As shown in Fig. 9, the reaction rate of NBE was obtained by fitting the NBE concentration and reaction time, and then the reaction rate of oxetane was calculated according to Eq. (7).

According to Eqs. (8) and (9), the fitting curves of $\ln(S \times r_{\text{NBE}})$ *versus* $\ln(C_{\text{NBE}})$ and $[\ln(S \times r_{\text{NBE}}) - \alpha \times \ln(C_{\text{NBE}})]$ *versus* $\ln(C_{\text{CHO}})$ are shown in Fig. 10(a) and (b), whose slopes represent the reaction series and intercepts represent the natural logarithm of the reaction rate constant (K*). Based on the fitting results, when the light intensity is 130 mW·cm^{-2}, the reaction orders of NBE (α) and CHO (β) are 0.4280 and 0, respectively, and the reaction rate constant is 0.1477 mol$^{0.428}$·L$^{-0.572}$·h^{-1}, so the reaction rate equation under this condition was established as follows:

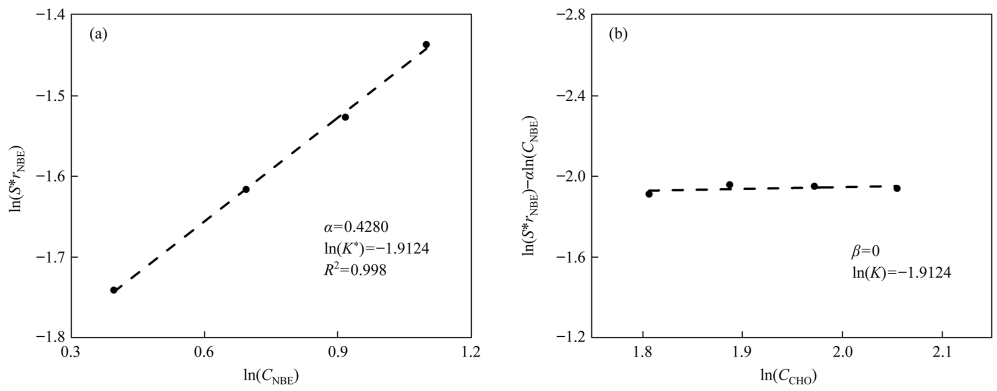

Fig. 10. (a) Fitting curves of $\ln(r_{\text{oxetane}})$ *versus* $\ln(C_{\text{NBE}})$, and (b) $[\ln(S \times r_{\text{NBE}}) - \alpha \times \ln(C_{\text{NBE}})]$ *versus* $\ln(C_{\text{CHO}})$ (130 mW·cm^{-2}, 20 °C, 10 h).

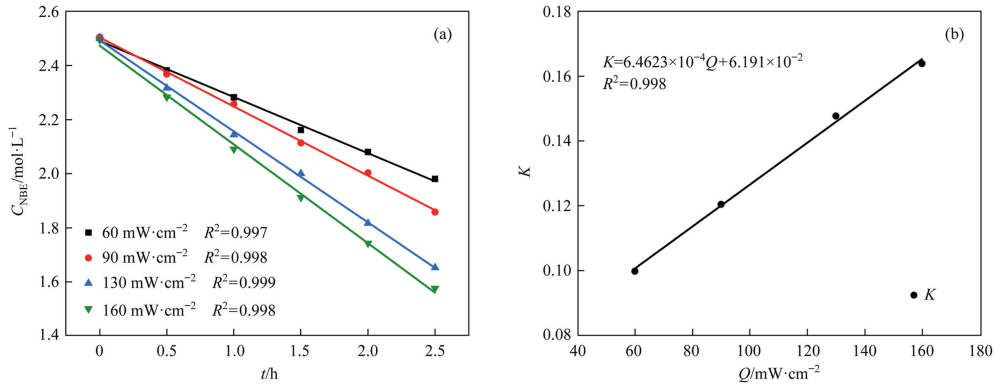

Fig. 11. (a) Fitting plots of the NBE concentration and reaction time at different light intensities; and (b) fitting curves of reaction rate constant and light intensity (20 °C, 10 h).

Table 1
Reaction rate constants and reaction series for different light intensities

Q/mW·cm^{-2}	K	α	β	R^2
160	0.1639	0.4143	0	0.998
130	0.1477	0.4280	0	0.999
90	0.1205	0.4265	0	0.998
60	0.0998	0.4131	0	0.997

$$r_{\text{oxetane}} = 0.1477 \times C_{\text{NBE}}^{0.4280} \quad (10)$$

The reaction rate constant (K) and the reaction series at different light fluxes can be obtained according to the above method, as shown in Fig. 11(a) and Table 1.

Table 2
Transposed Paternò-Büchi reaction between biomass ketones and alkenes

Entry	Alkene	Ketone	Structure of Oxetane	Conversion of alkene/%	Conversion of ketone/%	Selectivity of oxetane/%
1①		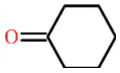	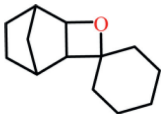	85.7	18.0	76.4
2①		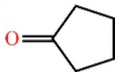	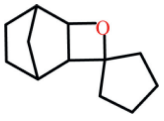	94.7	20.7	82.8
3①		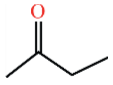	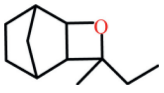	85.8	13.7	55.5
4②			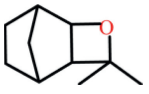	98.7	19.9	58.9
5①		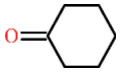	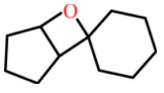	13.3	2.1	19.4
6①		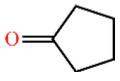	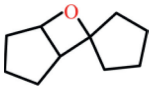	11.0	2.7	32.0
7②			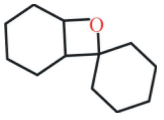	12.7	2.2	8.5
8②			–	100.0	–	–

① Photosensitizer is AP (10% (mol) of alkene), the molar ratio of alkenes and ketone is 1: 4, 10 h, 20 °C, 130 mW·cm^{-2}.
② Photosensitizer is AP (10% (mol) of alkene), the molar ratio of alkenes and acetone is 1: 10, 10 h, 20 °C, 130 mW·cm^{-2}.

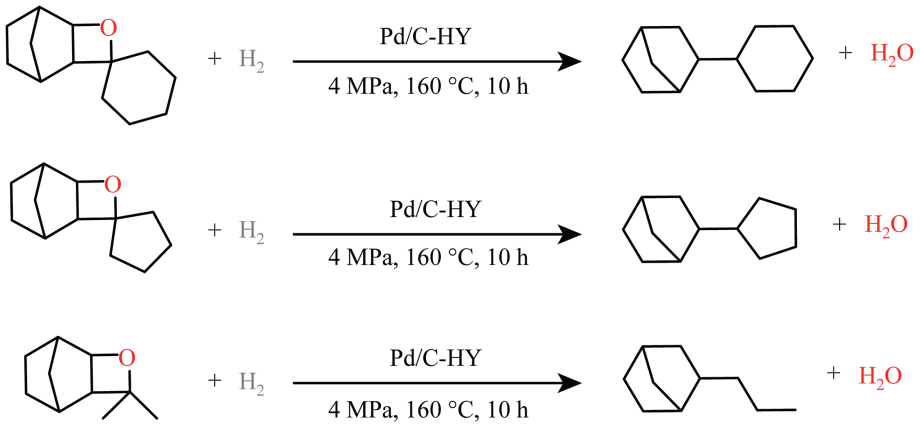

Fig. 12. The hydrogenation deoxygenation reaction equation of NBE + CHO-Oxe, NBE + CPO-Oxe and NBE + ATO-Oxe.

As the light flux increases, the reaction rate constant increases linearly. The reaction rate equation of the combined concentration and light flux can be characterized by Eq. (11).

$$r_{\text{oxetane}} = \left(6.4623 \times 10^{-4} \times Q + 6.191 \times 10^{-2}\right) \times C_{\text{NBE}}^{0.4205\pm0.01} \tag{11}$$

The transposed Paternò-Büchi reaction was also applied for several biomass-derived ketones and cyclic alkenes. As shown in Table 2, the reactions of NBE and cyclic ketone or alkyl ketone (with AP as a photosensitizer) show a higher reaction efficiency (NBE conversions are more than 85%), which also delivers the relatively high selectivity of the oxetane product. Notably, cyclic ketone as the reactant (Entry 1,2) shows higher oxetane product selectivity than that of alkyl ketone (Entry 3,4), because the latter is more prone to the intermolecular cycloaddition reaction of NBE (the main byproduct is PCTD). In addition, cyclopentene and cyclohexene can also react with cyclic ketone (Entry 5,6) or alkyl ketone (Entry 7) to form oxetane, but the conversion rate is low because the high triplet energy (which is influenced by the degree of conjugation of the compounds) reduces the efficiency of energy transfer [28]. Cyclohexadiene (Entry 8) with a greater degree of conjugation is almost completely converted to its own [2 + 2] cycloaddition product; the oxetane product is not detected, possibly due to the lower triplet energy (54 kcal·mol^{-1}).

In conclusion, the selection of photosensitizer and alkene substrates is the key to the transposed Paternò-Büchi reaction. The oxetane selectivity of cyclic ketones is better than that of alkyl ketones, and the alkenes with higher conjugation have lower triplet energy, which leads to more efficient triplet energy transfer.

3.5. Fuel properties

The oxetane product generated by the reaction of NBE with CHO (named NBE + CHO-Oxe) was hydrodeoxidized (Fig. 12) and purified to obtain the new hydrocarbon fuel with a purity higher than 95% (with trace ring-opening byproducts). As shown in Fourier transform infrared (FT-IR) spectra (Fig. S6), NBE + CHO-Oxe shows the absorption peaks at 1267 cm^{-1} and 1157 cm^{-1}, referring to the stretching vibration peaks of C—O—C bonds [31], and the peaks at 989 cm^{-1} and 823 cm^{-1} are antisymmetric and symmetric deformation vibration peaks of C—O—C bonds [32]. After the HDO reaction, the above peaks disappeared, indicating the oxygen atoms were removed successfully. The mass spectrum of the HDO product (NBE + CHO-Oxe-HDO) is shown in Fig. S7, which further confirms the production of saturated hydrocarbon fuel. Using the same treatment, the other two fuels were generated from NBE + CPO-Oxe and NBE + ATO-Oxe, respectively (Fig. 12), with their mass spectra shown in Fig. S8. Remarkably, according to the mass spectrometry (Fig. S8) and nuclear magnetic resonance (NMR) characterization (Fig. S13), NBE-ATO-Oxe tends to form 2-*n*-propylbicyclo[2.2.1]heptane rather than 2-isopropylbicyclo[2.2.1]heptane after HDO reaction, which may be due to the hydrogenation isomerization [33]. Therefore, the fuels, namely 1#, 2#, and 3#, from NBE + CHO-Oxe, NBE + CPO-Oxe, and NBE + ATO-Oxe, were obtained, and their physicochemical properties were tested and listed in Table 3. With the bridged carbon structures, 1#, 2#, and 3# fuels show much higher density and NHOC than bicyclohexane, bicyclopentane, and isopropyl-cyclohexane with similar molecule structures. Meanwhile, the as-synthesized fuels show a low freezing point (<−55 °C) and low viscosity. Especially for 2# and 3# fuel, their −40 °C viscosity values are as low as 26.17 and 10.67 mPa·s, respectively.

Table 3
Properties of fuels synthesized *via* transposed Paternò–Büchi reaction and other fuels

Fuel		1#	2#	3#	Bicyclopentane	Isopropyl-cyclohexane	Bicyclohexane
Structure		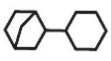	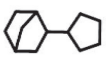	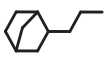	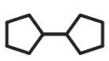		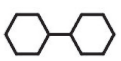
Density (20 °C)/g·ml^{-1}		0.938	0.928	0.864	0.867	0.802	0.887
NHOC/MJ·kg^{-1}		42.50	42.53	42.60	42.42	43.4	42.97
NHOC/MJ·L^{-1}		39.87	39.47	36.80	36.78	34.81	38.11
Viscosity/mPa·s	25 °C	–	–	–	1.62	1.0 (45 °C)	3.72
	20 °C	7.08	3.79	2.05	4.60 (35 °C)	–	–
	0 °C	14.82	6.11	3.08	–	–	6.33 (5 °C)
	−20 °C	41.61	11.44	5.27	–	–	–
	−40 °C	213.41	26.17	10.67	–	–	–
Freezing point/°C		<−55	<−55	<−55	−38.0	–	1.2
Ref.		This work	This work	This work	[34]	[35]	[5]

4. Conclusions

In this work, HED fuels with high density and excellent cryogenic properties have been synthesized by the photoinduced transposed Paternò-Büchi reaction of biomass-derived ketones and NBE. The reaction, mechanism including photosensitizer excitation, triplet energy transfer, cyclization, and relaxation, is verified by the triplet-energy quenching result, phosphorescence quenching result, and DFT calculation. The photosensitizer type and addition, NBE/CHO molar ratio, reaction temperature, and incident light flux are optimized, and the NBE conversion reaches 85.7%, with the oxetane yield higher than 65%. Then, the reaction kinetics of $r_{\text{oxetane}} = (6.4623 \times 10^{-4} \times Q + 6.191 \times 10^{-2}) \times C_{\text{NBE}}^{0.4205 \pm 0.01}$ are obtained. Meanwhile, changing the photosensitizers and alkene substrates expands the idea of substrate selection for the transposed Paternò-Büchi reaction. Importantly, the obtained HED fuels show high density and NHOC, as well as low freezing point and viscosity, which are promising to serve as high-performance jet fuels, and their total yields are higher than 65%, which is comparable to that of bio-JP-10 [36], but subsequent optimization of the process conditions and an increase in yield are still needed to meet the demands of industrial production.

Declaration of Interest

The authors declare that they have no known competing financial interests or personal relationships that could have appeared to influence the work reported in this paper.

Data Availability

Data will be made available on request.

Acknowledgements

The authors appreciate the support from National Key Research and Development Program of China (2021YFC2103704), the National Natural Science Foundation of China (22222808, 21978200), and the Haihe Laboratory of Sustainable Chemical Transformations.

Supplementary Material

Supplementary data to this article can be found online at https://doi.org/10.1016/j.cjche.2023.09.014.

References

[1] X.W. Zhang, L. Pan, L. Wang, J.J. Zou, Review on synthesis and properties of high-energy-density liquid fuels: Hydrocarbons, nanofluids and energetic ionic liquids, *Chem. Eng. Sci.* 180 (2018) 95–125.
[2] G.K. Nie, X.W. Zhang, P.J. Han, J.J. Xie, L. Pan, L. Wang, J.J. Zou, Lignin-derived multi-cyclic high density biofuel by alkylation and hydrogenated intramolecular cyclization, *Chem. Eng. Sci.* 158 (2017) 64–69.
[3] J.J. Xie, X.W. Zhang, Y.K. Liu, Z. Li, E. Xiu-tian-feng, J.W. Xie, Y.C. Zhang, L. Pan, J. J. Zou, Synthesis of high-density liquid fuel *via* Diels-Alder reaction of dicyclopentadiene and lignocellulose-derived 2-methylfuran, *Catal. Today* 319 (2019) 139–144.
[4] L. Wang, X.W. Zhang, J.J. Zou, H. Han, Y.H. Li, L. Wang, Acid-catalyzed isomerization of tetrahydrotricyclopentadiene: Synthesis of high-energy-density liquid fuel, *Energy Fuels* 23 (5) (2009) 2383–2388.
[5] Q. Deng, G.K. Nie, L. Pan, J.J. Zou, X.W. Zhang, L. Wang, Highly selective self-condensation of cyclic ketones using MOF-encapsulating phosphotungstic acid for renewable high-density fuel, *Green Chem.* 17 (8) (2015) 4473–4481.
[6] B.G. Harvey, R.L. Quintana, Synthesis of renewable jet and diesel fuels from 2-ethyl-1-hexene, *Energy Environ. Sci.* 3 (3) (2010) 352–357.
[7] Q. Deng, P.J. Han, J.S. Xu, J.J. Zou, L. Wang, X.W. Zhang, Highly controllable and selective hydroxyalkylation/alkylation of 2-methylfuran with cyclohexanone for synthesis of high-density biofuel, *Chem. Eng. Sci.* 138 (2015) 239–243.
[8] S.S. Li, F. Chen, N. Li, W.T. Wang, X.R. Sheng, A.Q. Wang, Y. Cong, X.D. Wang, T. Zhang, Synthesis of renewable triketones, diketones, and jet-fuel range cycloalkanes with 5-hydroxymethylfurfural and ketones, *ChemSusChem* 10 (4) (2017) 711–719.
[9] S.S. Li, N. Li, W.T. Wang, L. Li, A.Q. Wang, X.D. Wang, T. Zhang, Synthesis of jet fuel range branched cycloalkanes with mesityl oxide and 2-methylfuran from lignocellulose, *Sci. Rep.* 6 (2016) 32379.
[10] Z.P. Huang, Z.T. Zhao, C.F. Zhang, J.M. Lu, H.F. Liu, N.C. Luo, J. Zhang, F. Wang, Enhanced photocatalytic alkane production from fatty acid decarboxylation via inhibition of radical oligomerization, *Nat. Catal.* 3 (2) (2020) 170–178.
[11] N.C. Yang, M. Nussim, M.J. Jorgenson, S. Murov, Photochemical reactions of carbonyl compounds in solution the Paterno-Büchi reaction, *Tetrahedron Lett.* 5 (48) (1964) 3657–3664.
[12] M. Fréneau, N. Hoffmann, The Paternò-Büchi reaction—Mechanisms and application to organic synthesis, *J. Photochem. Photobiol., C* 33 (2017) 83–108.
[13] G. Büchi, C.G. Inman, E.S. Lipinsky, Light-catalyzed organic reactions. I. the reaction of carbonyl compounds with 2-methyl-2-butene in the presence of ultraviolet light, *J. Am. Chem. Soc.* 76 (17) (1954) 4327–4331.
[14] F.H. Isikgor, C.R. Becer, Lignocellulosic biomass: a sustainable platform for the production of bio-based chemicals and polymers, *Polym. Chem.* 6 (25) (2015) 4497–4559.
[15] D.M. Alonso, J.Q. Bond, J.A. Dumesic, Catalytic conversion of biomass to biofuels, *Green Chem.* 12 (9) (2010) 1493.
[16] H.B. Schlegel, Optimization of equilibrium geometries and transition structures, *J. Comput. Chem.* 3 (2) (1982) 214–218.
[17] S. Wilsey, L. González, M.A. Robb, K.N. Houk, Ground- and excited-state surfaces for the[2+2]-photocycloaddition of α, β-enones to alkenes, *J. Am. Chem. Soc.* 122 (24) (2000) 5866–5876.
[18] Y. Liu, Y. Chen, S. Ma, X.L. Liu, X.W. Zhang, J.J. Zou, L. Pan, Synthesis of advanced fuel with density higher than 1 g/mL by photoinduced[2 + 2] cycloaddition of norbornene, *Fuel* 318 (2022) 123629.
[19] R. Remy, C.G. Bochet, Arene–alkene cycloaddition, *Chem. Rev.* 116 (17) (2016) 9816–9849.
[20] R.S.H. Liu, N.J. Turro Jr., G.S. Hammond, Mechanisms of photochemical reactions in solution. XXXI. activation and deactivation of conjugated dienes by energy transfer, *J. Am. Chem. Soc.* 87 (15) (1965) 3406–3412.
[21] K. Nakatani, H. Sato, R. Fukuda, A catalyzed *E/Z* isomerization mechanism of stilbene using *para*-benzoquinone as a triplet sensitizer, *Phys. Chem. Chem. Phys.* 24 (3) (2022) 1712–1721.
[22] P.J. Wagner, Conformational changes involved in the singlet-triplet transitions of biphenyl, *J. Am. Chem. Soc.* 89 (12) (1967) 2820–2825.
[23] J. Bull, O. Davis, Recent advances in the synthesis of 2-substituted oxetanes, *Synlett* 26 (10) (2015) 1283–1288.
[24] M. Zhu, X.A. Zhang, C. Zheng, S.L. You, Visible-light-induced dearomatization *via*[2+2]cycloaddition or 1, 5-hydrogen atom transfer: Divergent reaction pathways of transient diradicals, *ACS Catal.* 10 (21) (2020) 12618–12626.
[25] N. El Achi, F. Gelat, N.P. Cheval, A. Mazzah, Y. Bakkour, M. Penhoat, L. Chausset-Boissarie, C. Rolando, Sensitized[2 + 2]intramolecular photocycloaddition of unsaturated enones using UV LEDs in a continuous flow reactor: Kinetic and preparative aspects, *React. Chem. Eng.* 4 (5) (2019) 828–837.
[26] A. Cuppoletti, J.P. Dinnocenzo, J.L. Goodman, I.R. Gould, Bond-coupled electron transfer reactions: Photoisomerization of norbornadiene to quadricyclane, *J. Phys. Chem. A* 103 (51) (1999) 11253–11256.
[27] C. Shen, M.J. Shang, H. Zhang, Y.H. Su, A UV-LEDs based photomicroreactor for mechanistic insights and kinetic studies in the norbornadiene photoisomerization, *AlChE. J.* 66 (2) (2020) e16841.
[28] W. Nau, Modern molecular photochemistry of organic molecules, in: N.J. turro, V. ramamurthy, J.C. scaiano (Eds.), ChemPhysChem (12) (13) (2011) 2496–2497.
[29] C. Prentice, A.E. Martin, J. Morrison, A.D. Smith, E. Zysman-Colman, Benzophenone as a cheap and effective photosensitizer for the photocatalytic synthesis of dimethyl cubane-1, 4-dicarboxylate, *Org. Biomol. Chem.* 21 (16) (2023) 3307–3310.
[30] F. Bayrakçeken, Triplet-triplet optical energy transfer from benzophenone to naphthalene in the vapor phase, *Spectrochim. Acta* 71 (2) (2008) 603–608.
[31] M. Arslan, O. Ceylan, R. Arslan, M.A. Tasdelen, Facile UV-induced covalent modification and crosslinking of styrene-isoprene-styrene copolymer *via* paterno-Büchi[2 + 2]photocycloaddition, *RSC Adv.* 11 (15) (2021) 8585–8593.
[32] N.K. Singha, B. de Ruiter, U.S. Schubert, Atom transfer radical polymerization of 3-ethyl-3-(acryloyloxy)methyloxetane, *Macromolecules* 38 (9) (2005) 3596–3600.
[33] E. Blomsma, J.A. Martens, P.A. Jacobs, Mechanisms of heptane isomerization on bifunctional Pd/H-beta zeolites, *J. Catal.* 159 (2) (1996) 323–331.
[34] J.F. Yang, N. Li, G.Y. Li, W.T. Wang, A.Q. Wang, X.D. Wang, Y. Cong, T. Zhang, Synthesis of renewable high-density fuels using cyclopentanone derived from lignocellulose, *Chem. Commun.* 50 (20) (2014) 2572–2574.
[35] Z.Y. Wu, Y.B. Mao, M. Raza, J.Z. Zhu, Y. Feng, S.X. Wang, Y. Qian, L. Yu, X.C. Lu, Surrogate fuels for RP-3 kerosene formulated by emulating molecular structures, functional groups, physical and chemical properties, *Combust, Flame* 208 (2019) 388–401.
[36] G.Y. Li, B.L. Hou, A.Q. Wang, X.L. Xin, Y. Cong, X.D. Wang, N. Li, T. Zhang, Making JP-10 superfuel affordable with a lignocellulosic platform compound, *Angew. Chem. Int. Ed.* 58 (35) (2019) 12154–12158.